Sentinels4Carbon (Sense4Fire)

Sentinel-based fuel, fire and emissions products to constrain the changing role of vegetation fires in the global carbon cycle

ESA Contract Number: 4000134840/21/I-NB

Algorithm Theoretical Baseline Document Version 3

(ATBDv3)

3 May 2024, Version 3

Prepared by:

Matthias Forkel, Christine Wessollek, Daniel Kinalczyk, Christopher Marrs

TUD Dresden University of Technology, Faculty of Environmental Sciences, Dresden, Germany

Vincent Huijnen, Jos de Laat

Royal Netherlands Meteorological Institute (KNMI), De Bilt, The Netherlands

Niels Andela, Dave van Wees

BeZero Carbon Ltd., London, UK

Contents

Figures

Tables

1 Introduction

This Algorithm Theoretical Baseline Document (ATBD) describes the methods and required input datasets that are developed within the ESA-funded Sense4Fire project: Sentinel-based fuel, fire and emissions products to constrain the changing role of vegetation fires in the global carbon cycle. The aim of Sense4Fire is to increase the scientific understanding of fire dynamics and their role in the carbon cycle by integrating observations from the Sentinels into new Earth observation products. We understand fire dynamics as all processes that contribute to pre-fire conditions of the land surface (i.e. fuel loads and fuel moisture), fire behaviour (fire ignitions, spread, speed, size, burned area, thermal emissions and radiative power), combustion and production of fire emissions (combustion completeness, combustion efficiency, biomass burning and composition of emissions) and the effect of fire emissions on atmospheric composition (injection height, smoke plumes, atmospheric gas composition, aerosols).

This third version of the ATBD (ATBDv3) is an update of the second version of the ATBD (ATBDv2.1) from 05.05.2023 (Forkel et al., 2023b). ATBDv3 provides for each of the approaches applied in Sense4Fire a list of updates. For a full description of each approach, please refer to ATBDv2.1. ATBDv3 includes additionally an assessment of requirements and needs to apply the approaches in near-real time.

ATBDv3 is accompanied with the second version of the Product Validation Report (PVRv3) (Forkel et al., 2024), which presents validation and inter-comparison results for each study region.

This document first provides an overview of the study regions and test areas (Chapter 2) and then provides updates for the three different approaches that are developed and applied in Sense4Fire to estimate fire emissions:

- **GFA-S4F** is based on the Global Fire Atlas (GFA) algorithm (Andela et al., 2019, 2022) and uses observations of active fires from the VIIRS and Sentinel-3 SLSTR instruments with a new fire type map to estimate fire emissions (Chapter 3).
- **TUD-S4F** is a new data-model fusion approach that combines several datasets from Sentinel-3 and other Earth observation products to estimate fuel loads, fuel moisture, fuel consumption, and fire emissions. (Chapter 4)
- **KNMI-S5p** is based on observation from Sentinel-5p, whereby fire emissions of CO and NOx are estimated using top-down approaches. These approaches serve as top-down estimates of regional total fire emissions (Chapter 5).

2 Spatial and temporal domain and study areas

2.1 Study regions and test areas

Our study domain covers four regions: South America (Amazon and Cerrado), Europe (southern Europe), southern Africa and Siberia. Within these study regions, we applied the approaches to three smaller test areas that include a range of representative land cover and fire types (Table 1). The test areas include a transect from frequently burning tropical forests to savannah in Brazil, an area with small agricultural and large savannah fires in southern hemisphere Africa, Mediterranean ecosystems in southern Europe, and a boreal forest to tundra region in Eastern Siberia. A more detailed description of the test areas can be found in ATBDv2.1.

Table 1: Overview about the study regions (large) and test areas (small).

Study region or test area	East/West extent	North/South extent
South America (Amazon/Cerrado) study region	40°W - 80°W	25°S - 10°N
Amazon test area	50°W - 55°W	9°S - 14°S
Europe study region	10°W – 29.5°E	34.5°N - 49°N
Southern Africa study region	10°E - 30°E	5°S - 25°S
Southern Africa test area	23°E - 28°E	11°S - 16°S
Siberia test area	132°E - 138°E	60°N - 71°N

For each test area, we apply all approaches in Sense4Fire to the fire season 2020 for atmospheric modelling purposes and to compare all approaches. Fire activity can vary considerably from year-to-year and 2020 was found to be of particular interest for the selected regions (e.g., extensive drought driven understorey fires in Brazil, and large forest fires in Eastern Russia). Individual approaches in Sense4Fire are additionally applied to other years.

3 GFA-S4F: Fire emissions from fire types

3.1 Summary and updates of the approach since ATBDv2.1

Since the previous ATBDv2.1 our focus has been on expanding and improving the approach for the African, European, and Siberian regions as well as enabling our approach to be run for any year from 2019 onwards and in near-real time. For South America we have now archived historic time-series from 2019 - 2023 and data are available in near-real time here https://amzfire.servirglobal.net/. For other regions only the year 2020 has been processed to date, but we have tested the approach for early 2024 ahead of our near-real time trial.

3.2 Setup for each study region

Our original approach presented in the ATBDv2.1 focused on the Amazon region, with exploratory work being carried out for other regions. We have now harmonized the data for regions outside the Amazon, including Siberia, Europe, and southern hemisphere Africa, based on a single approach and globally (for each region) consistent data product. Providing data as a single data product simplifies data sharing with partners, like KNMI, and is a first step towards a global emissions product. Broadly speaking, the GFA.S4F approach includes five steps: (i) mapping of individual fire events, (ii) creation of attribute table for each fire object, including fire types, (iii) estimation of burned area, (iv) estimation of conversion factors and calculation of fuel consumption, and (v) calculation of trace gas emissions. Here we provide a short summary of updates in each of these areas.

In the first step we identify individual fire events. The algorithm to track individual fire events is consistent for all four study regions, the Amazon, southern hemisphere Africa, Europe, and Siberia, and detailed in ATBDv2.1. More recently, we have added the optional inclusion of Sentinel-3 data for all regions except the Amazon (Table 2).

Table 2: Overview of datasets used in the GFA.S4F approach in study region.

Study region	Fire types	Active fire data	Scaling factor for burned area
South America	Understory forest fires Savanna fires Deforestation fires Small land clearings and agricultural fires	VIIRS (NOAA20, SNPP)	Burned area scaling of deforestation and savanna and grassland fires based on MCD64A1. Small fires are scaled to 0.1 of the grid area (0.005 x 0.005 degree), and forest fire burned area is estimated to equal area identified by active fire detections.
Europe, Southern Africa, Siberia	Boreal forest fires Temperate forest fires Tropical forest fires Savanna and grassland fires Cropland fires	VIIRS (NOAA20, SNPP) Sentinel-3 SLSTR (Sentinel-3 A and B)	No scaling applied, burned area is estimated as the area within all grid cells that had active fire detections on a global 0.005-degree grid.

In the second step we construct an attribute table for each fire event including information on fire behaviour, land cover and fire type. Outside the Amazon region, we now identify five fire types, including boreal forest fires, temperate forest fires, tropical forest fires, grassland and savannah fires and cropland fires based on region and land cover information from WorldCover-2 (Table 2). Characteristics on the behaviour of the fire include the duration, radiative power, and fire affected area.

In the third step we map burned area. So far, no scaling factors have been applied outside the Amazon, and burned area is estimated as the total pixel area of all pixels that contained active fire detections on a global 0.005° grid (Table 2). Evaluation of this approach against Sentinel-2 data highlights that active fire detections provide accurate estimates of burned area for forest and deforestation fires, but not for savannah, grassland, or cropland fires (see PVR2.1). Additional comparison against burned area estimates from GFED5 are also encouraging (see PVRv3). Nevertheless, we are still aiming to calibrate burned area for savanna and cropland fires against the Sentinel-2 FireCCI burned area product for Africa, as these are regionally important fire types.

In the fourth step we estimate fuel consumption for each fire event based on fire type specific conversion factors. Conversion factors translate the observed fire radiative power (MW) per area burned (m^2) to fuel consumption per area burned (g C m^{-2}). For fuel consumption, we rely on the dataset of fuel consumption observations compiled by van Wees et al. (2022). For each fire type, we reviewed the database to include the most relevant field observations of fuel consumption (ton C ha^{-1}) and match these to the distribution fire radiative power per area burned (MW ha^{-1}) using the approach explained in the ATBDv2.1.

In the fifth step we convert carbon to trace gas emissions. We review emissions factors compiled by Andrea et al. (2019) to derive fire type specific emissions factors of CO, summarised in Table 3. For the fire types we consider, we noticed that the standard deviation of CO emissions factors ranged between 10 to 30% of absolute values, and we therefore expect that the uncertainty arising from emissions factors is likely smaller than the uncertainty introduced by conversion factors.

Table 3: Overview of emissions factors used in the GFA.S4F approach.

Fire type	**CO2 g kg^{-1}**	**CO g kg^{-1}**	**NOx (NO) g kg^{-1}**
Deforestation fires	1641	95.5	1.7
Tropical forest fires	1510	104.0	2.0
Small clearing and agricultural fires	1431	76.2	2.4
Temperate forest fires	1647	88.0	1.9
Boreal forest fires	1489	127.0	0.9
Savanna and grassland fires	1656	69.2	2.5
Cropland fires	1585	102	3.1

Given the importance of accurate conversion factors and limited field observations of fuel consumption in certain areas, we plan to further calibrate conversion factors by fire type using TROPOMI data as reference (Fig. 1). For this approach, we ingest the GFA.S4F fire CO emissions estimates in the IFS COMPO atmospheric model for each fire type separately, to derive daily modelled contributions to total CO column concentrations from each fire type. Initially, KNMI has provided data based on this approach for August-September 2020 in the southern Amazon. In our first experiment (Fig. 1), we included all four fire types and background CO concentrations simultaneously in a multiple linear regression using:

$$\mathrm{TROPOMI\ CO\ retrieval} = a \cdot \mathrm{CO}_{\mathrm{deforestation}} + b \cdot \mathrm{CO}_{\mathrm{forest}} + c \cdot \mathrm{CO}_{\mathrm{savanna}} + d \cdot \mathrm{CO}_{\mathrm{small}} + e \cdot \mathrm{CO}_{\mathrm{background}}.$$

This resulted in significant overfitting (with a = 0.55, b = 0.50, c = 3.30, d = -1.87, and e=1.26), particularly for small emissions contributions like those from small clearing and agricultural fires (CO_{small}). However, a simpler model separating forest from savannah and grassland fires:

$$\text{CO TROPOMI} = a \cdot (CO_{deforestation} + CO_{forest} + d \cdot CO_{small}) + b \cdot (CO_{savanna} + CO_{background}),$$

resulted in more realistic (a = 0.69, b = 1.28) emissions adjustments while still improving r^2 values from 0.74 to 0.80. Interestingly, both experiments suggest a relative overestimate of forest fire emissions and underestimate of savannah and grassland emissions in South America by our approach. We further explored this concept using a larger set (full year) of GFAS data prepared by KNMI for a separate project and found significant improvements (reductions in overfitting) when considering a larger spatiotemporal domain. We therefore believe that this may be a helpful approach to constrain conversion factors in areas where limited field observations are present, like the humid tropics of Africa. For this purpose, we have already expanded the GFA.S4F approach to include all of southern hemisphere Africa (0-35° south).

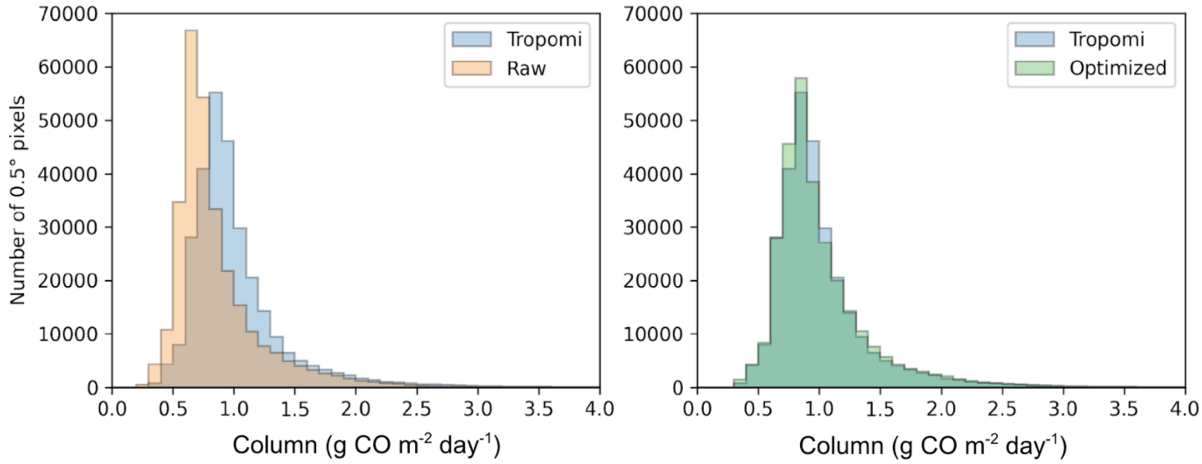

Figure 1: Distribution of CO column concentrations from our model and TROPOMI before and after optimization according to the first experiment.

3.3 Requirements and feasibility for near-real time application

The GFA.S4F approach is now ready to provide twice monthly updates on fire emissions during our near-real time emissions experiment in summer 2024, with the option of more frequent updates during fire emergencies in Europe, southern hemisphere Africa, or Siberia. We made several adjustments to our code to prepare for these near-real time updates, as explained below. Note that emissions estimates for the Amazon region are already "operationally" available in near-real time with a lag of about one day (https://amzfire.servirglobal.net/).

The optional inclusion of Sentinel-3 data and "on the fly" calibration of conversions factors was originally included to enable near-real time emissions estimates, as Sentinel-3 data were not available in near-real time. This is now no longer required, as Sentinel-3 data are now provided at short latency. Nevertheless, we have maintained this helpful feature that also allows for future inclusion of updated or expanded (e.g. S3 daytime) active fire detection products from ESA and NASA. This could also be further expanded to include data from different sensors available for different periods in the future, e.g. in case of instrument failures or additions.

Harmonizing fire types, conversion factors, and emissions factors and combining the approaches for the various study regions into a single Github repository and pipeline was another key step that enables the creation of near real-time emissions estimates for all study regions. This step also provides data to project partners in an accessible and consistent format.

Finally, we updated “static” files (updated annually) for the Amazon dashboard approach, including the removal of e.g. static sources of active fire detections (e.g. industry) and recent forest loss and deforestation events to provide 2024 emissions estimates.

4 TUD-S4F: Fire emissions from a data-model fusion approach for fuel loads, fuel moisture content and combustion

4.1 Summary of the approach

The TUD.S4F approach uses data-model fusion approaches and satellite-derived on various vegetation metrics like tree and herbaceous fractional coverage, leaf area index (LAI), as well soil water index (SWI), and burned area. From these inputs, it generates estimations for fuel load and moisture dynamics over time, combustion completeness, fuel consumption, combustion efficiency, emission factors, and fire emissions (Figure 22).

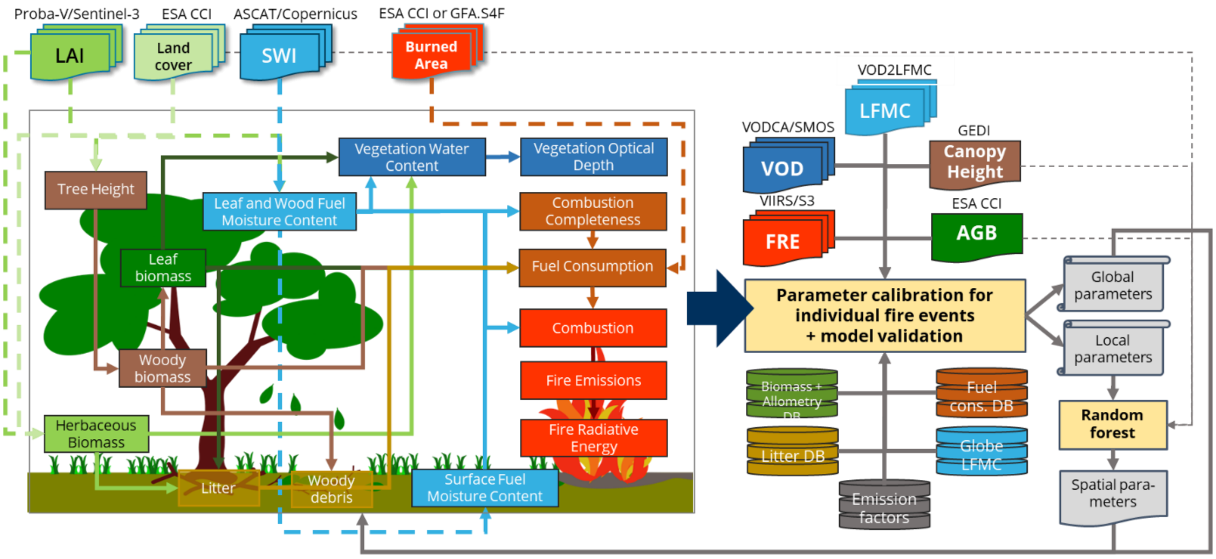

Figure 2: Simplified structure of the TUD.S4F approach to estimate fuel and combustion dynamics with satellite dataset used as forcing (top) and further datasets used for parameter calibration and model validation (right).

The model accounts for diverse fuel components including tree leaves, branches, stems, herbaceous vegetation, surface litter, and fine and coarse woody debris (FWD, CWD). Fuel loads are calculated based on canopy height and LAI, employing allometric equations to estimate biomass in tree components (Falster et al., 2015). Surface fuel accumulation is then estimated accounting for land cover changes and temporal variations in LAI, influencing turnover rates of herbaceous and leaf biomass, FWD, and CWD, respectively. Fuel moisture content (FMC) is derived from SWI and LAI for live vegetation (LFMC) and from SWI for woody biomass. SWI serves as a surrogate for surface fuel moisture content. Estimated FMC is then used to compute combustion completeness based on a linear relationship. The model also computes vegetation water content (VWC) from FMC and biomass, facilitating comparison and calibration against satellite observations of vegetation optical depth (VOD).

In contrast to conventional fire emission inventories, TUD.S4F dynamically calculates emission factors based on fuel components and moisture levels using a chemical-based combustion model (Rego et al., 2021). Calibration involves comparing the combustion model against the emission factor database from Andreae (2019) and fire radiative energy.

A detailed description of the model approach is provided in ATBDv2.1 and is still valid for ATBDv3 and the results presented in PVRv3. The only modification for ATBDv3 and PVRv3 is in the computation of surface fuels by additionally accounting for biomass extraction by harvest (i.e. wood extraction through deforestation or harvest of crops) before the turnover is entering the surface litter, FWD and CWD pools. For the turnover of woody and herbaceous vegetation, we account for a fraction being removed from the ecosystem through harvest, thus bypassing the woody debris and litter pools, respectively. Regarding tree trunks and large branches (with diameter > 7.62 cm), we assume a reduction in the harvest index (HI) from maximum 0.8 (HI_{max}) at a tree cover of 15% to HI = 0.5 at a tree cover of 100%. This implies that regions with lower tree cover (like forest edges or savannah areas) experience a higher fraction of woody harvest compared to regions with dense forest cover (such as intact tropical forests). We presume that small branches (with diameter < 7.62 cm) always contribute to the fine woody debris pool. For herbaceous vegetation, we consider harvest only in croplands, with the harvest index increasing from 0 at 0% cropland cover to 0.5 at 100% cropland cover. This implementation of harvest helps to reduce regional biases in estimated surface fuel loads in comparison with the field data compiled by van Wees (van Wees et al., 2022). All TUD.S4F results from Version 0.2 onwards that are included in the Experimental Database include this implementation of harvest. We therefore recommend to not further use results with Version 0.1 from the Experimental Database.

The changes in ATBDv3 further include a minor bug fix in the computation of emission factors. However, this bug fix does not significantly affects the computation of fire emissions.

4.2 Setup for each study region

In ATBDv3 and PVRv3, we applied the TUD.S4F approach with the same input data as it was done in ATBDv2.1. The datasets that are used in the TUD.S4F approach are summarised in Table 4.

The only difference is in the application of TUD.S4F for the Siberia study region because the GEDI L3 gridded canopy height (rh100) is not available for latitudes > 52°N. Hence we used as an alternative the global canopy height dataset from ETH Zurich (Lang et al., 2023). This dataset is also based on observations by GEDI but applies a deep learning model with Sentinel-2 observations to extrapolate GEDI canopy height observation globally.

Table 4: Overview of datasets used in the TUD-S4F approach.

Variables	Dataset (Sensor)	Spatial resolution and coverage	Temporal resolution and coverage	Use in the TUD.S4F approach	Source
fCOVER, LAI	Sentinel-3/OLCI and Proba-V	333 m, global	10 daily, Jan/2014 – Oct/2021 (281 observations)	Forcing for tree canopy height, biomass, turnover and combustion completeness	https://land.copernicus.eu/global/products/lai (Fuster et al., 2020)
Land cover (f_{tree}, f_{herb}, f_{crop})	Land cover_cci	300 m, global	annual, 1992-2020	Forcing for tree height and biomass	https://www.esa-landcover-cci.org/?q=node/164
Above ground biomass (forests)	Biomass_cci	100 m, global	(1990s), 2010, 2017, 2018	Calibration	http://dx.doi.org/10.5285/bedc59f37c9545c981a839eb552e4084
Forest Canopy Height	GEDI L3 Gridded Land Surface Metrics (rh100)	1 km, global (52°N-52°S)	Composite from 2019-2021	Calibration (all regions except Siberia))	https://doi.org/10.3334/ORNLDAAC/1952
Forest Canopy Height	ETH Zurich data, extrapolated from GEDI	10 m, global	Year 2020	Calibration (only Siberia)	https://doi.org/10.3929/ethz-b-000609802 (Lang et al., 2023)
Ku/X/C-band Vegetation Optical Depth	VODCA VOD	0.25°, global	daily, 1987-2020 (depending on band)	Calibration	https://zenodo.org/record/2575599 (Moesinger et al., 2020)
L-band Vegetation Optical Depth	SMOS LPRM L-VOD	0.25°, global	daily, 2010-2020	Calibration	(van der Schalie et al., 2017)
Live-fuel moisture content	VOD2LFMC	0.25°, global	daily, 2000-2017	Calibration	https://doi.org/10.5281/zenodo.6545571 (Forkel et al., 2023a)
Live-fuel moisture content	Globe-LFMC	Measurements from field sites	Depending on site	Pre-calibration in LFMC calculation	(Yebra et al., 2019)
Soil water index	Metop-ASCAT	0.1°, global	10 daily, since 2007	Forcing for surface fuel moisture and woody moisture	https://land.copernicus.eu/global/products/swi
Burned area (baseline 2014-2019)	Fire_cci 5.1, MODIS	250 m, global	Monthly with first day of detection, used for the	Forcing for fuel consumption	https://dx.doi.org/10.5285/58f00d8814064b79a0c49662ad3af537 (Lizundia-Loiola et al., 2020)

			period 2014-2019		
Burned area (2020)	GFA.S4F burned area estimates derived from active fires (VIIRS, Sentinel-3)	500 m, study region	daily, 2020 used for year 2020	Forcing for fuel consumption	From GFA.S4F approach
Fire radiative energy	GFA.S4F FRE derived from active fires (VIIRS, Sentinel-3)	500 m, study region	daily, 2020	Calibration	From GFA-S4F approach
Tree allometry, biomass in tree components	BAAD	Measurements from single trees, laboratories and field sites	--	Pre-calibration for tree biomass	https://doi.org/10.6084/m9.figshare.c.3307692.v1 (Falster et al., 2015)
Fuel loads, fuel consumption, combustion completeness	Updated fuel consumption database	Measurements from field sites	--	Calibration Evaluation	(van Wees et al., 2022)
Litter pools	Global Database of Litterfall Mass and Litter Pool Carbon	Measurements from field sites	--	Evaluation	(Holland et al., 2014)
Emission factors, modified combustion efficiency	Emission factor database	In situ measure-ments and laboratories	--	Pre-calibration for combusiton Calibration	Andreae (2019)

We performed several experiments with TUD.S4F to quantify the effect of the used burned area data (all study regions) and of the computation of emission factors (South America only) on the estimated fire emissions (Table 5).

Table 5: Overview about factorial experiments with the TUD.S4F approach in each study region. All experiments cover the period 2014-2020.

Name	Study region	Fire data	Emission factors	TUD.S4F model version
TUD.S4F	South America	GFA.S4F	dynamic	V0.2
TUD.S4F.fixEF	South America	GFA.S4F	fixed	V0.2
TUD.S4F.FireCCI	South America	FireCCI51	dynamic	V0.2
TUD.S4F	Europe	GFA.S4F	dynamic	V0.2
TUD.S4F.FireCCI	Europe	FireCCI51	dynamic	V0.2
TUD.S4F	Southern Africa	GFA.S4F	dynamic	V0.2
TUD.S4F.FireCCI	Southern Africa	FireCCI51	dynamic	V0.2
TUD.S4F	Siberia	GFA.S4F	dynamic	V0.2

4.3 Requirements and feasibility for near-real time application

The inputs required for the near real-time (NRT) application are the 10-daily Soil Water Index (SWI) and the 10-daily Leaf Area Index (LAI), both provided by the Copernicus Global Landservice (CGLS), yearly ESA CCI Global Landcover (LC), and burned area from either GFA-S4F or from FireCCI (BA). The CGLS updates the SWI data in 6 post-processing stages over 60 days. The difference between the initial (RT0) product based on past observations and the post-processed, consolidated product (RT6) is the number of data points, with the RT0 product having significant data gaps. That means that observations at t = 0 are consolidated with 6 observations of t = 1, t = 2, […], t = 6. Therefore, the NRT application will be run two times, on the day of release with product RT0 and after 60 days when CGLS provides the RT6 product. As the provided LAI product uses the same post-processing regime, no further adjustments or model runs are needed. To satisfy the needs for an NRT application, LC and BA would be required in the same temporal resolution as the SWI and LAI CLGS products.

Table 6: Overview of the datasets which will be needed in temporal high resolution for the NRT application.

Dataset	Provided Temporal Resolution	Needed Temporal Resolution
CGLS LAI	10 days	10 days
CGLS SWI	10 days	10 days
ESA CCI Global Landcover	static	10 days
Burned Area	monthly	10 days

Furthermore, the current data structure has to change from combined time-series data to single observation imagery data, which would resemble the structure of the provided NRT data. In addition, an option to restart the TUD-S4F model based on previous model states of surface fuels is needed to calculate single timesteps. However, with the above changes, the NRT product should be available within a time lag of three days, starting with the availability of the required input datasets.

5 KNMI-S5p: Top-down constraints on fire emissions

5.1 Summary and updates of the approach since ATBDv2.1

For the previous ATBD (V2.1) and PVR (V2.1) reporting only a short time period was chosen (August-September 2020) for deriving and evaluating emissions against TROPOMI observations, using the approaches from BeZero and CAMS GFAS emission data as priori. The main focus region was the Amazon/Cerrado for which results were extensively analysed and discussed, as documented in de Laat et al. (2024). Some results were presented for the other study regions but with only a limited analysis.

Since then, the IFS-COMPO model version has been updated towards version CY49R1, implying improvements in the model description of various processes, together with updates to anthropogenic and biogenic background emissions. The approach has been extended for the entire year 2020, and also applied to other study regions as described in

Table 1. A set of IFS-COMPO simulations has been performed including configurations for the estimation of post-hoc fire emission optimization, and its evaluation.

5.2 Setup for each study region

The main IFS-COMPO experiments that have been executed for the evaluation of various emission estimates are listed in Table 3. Specifically, this includes experiments which apply either the GFAS and GFA-S4F CO and NO2 emissions, as well as one simulation which applies the optimized NOx emissions with GFA-S4F as priori. The KNMI.S5p CO emissions were only optimized for southern Africa, taking the GFA-S4F emissions as a priori. This was done using a mass balance method, and by assessing the simulation results when using the GFAS and the GFA-S4F emissions.

Table 7: Specification of IFS-COMPO experiments for evaluation and optimization of various emission inventories.

IFS-COMPO run (experiment ID)	Purpose	emissions	IFS-COMPO version
GFAS (b2hx)	Evaluation of GFAS CO and NOx emissions	GFASv1.4	CY49R1
GFA-S4F (b2il)	Evaluation of GFA-S4F CO and NOx emissions	GFA-S4F	CY49R1
KNMI.S5p (b2ip)	Evaluation of KNMI.S5p optimized CO and NOx emissions	KNMI.S5p	CY49R1

5.3 Requirements and feasibility for near-real time application

In future near-real applications of the Sense4Fire approaches, it is foreseen that the KNMI approaches do not represent an independent emission inventory but are used as tool to evaluate the GFA-S4F and TUD-S4F bottom-up emission estimates in near-real time.

IFS-COMPO model simulations will follow the NRT production of the bottom-up emissions, enabling a rapid assessment against TROPOMI observations of CO and NO2. Here we will use a standard IFS-COMPO model version (Cy49R1), setup in its default configuration with T511 horizontal resolution (~40 km), and 137 model levels, that is run for 24 hours, starting at 0h00 UTC, daily, initialized using Meteorology taken from the ECMWF operational analysis. These input data become available with about one day time lag.

Any emission input data will also be the same as used operationally, i.e. CAMS-GLOB-ANT anthropogenic emissions, CAMS-GLOB-BIO biogenic and CAMS-GLOB-SOIL soil NOx emissions. As one exception compared to the CAMS operational model configuration, we will adopt a configuration with tropospheric chemistry activated only. This is consistent with any other model simulations executed in the Sense4Fire framework.

A reference simulation will use the GFAS fire emissions for all emission trace gases, which can be compared to a second simulation that uses the GFA-S4F emissions for CO and NOx, as they come available to KNMI. We foresee weekly batches of emission updates, for the preceding week, which implies a time lag of about two-three weeks for the production of the NRT-evaluation results.

6 References

Andela, N., Morton, D. C., Giglio, L., Paugam, R., Chen, Y., Hantson, S., Van Der Werf, G. R., and Randerson, J. T.: The Global Fire Atlas of individual fire size, duration, speed and direction, Earth Syst. Sci. Data, 11, 529–552, 2019.

Andela, N., Morton, D. C., Schroeder, W., Chen, Y., Brando, P. M., and Randerson, J. T.: Tracking and classifying Amazon fire events in near real time, Sci. Adv., 8, eabd2713, https://doi.org/10.1126/sciadv.abd2713, 2022.

Andreae, M. O.: Emission of trace gases and aerosols from biomass burning–an updated assessment, Atmospheric Chem. Phys., 19, 8523–8546, 2019.

Falster, D. S., Duursma, R. A., Ishihara, M. I., Barneche, D. R., FitzJohn, R. G., Vårhammar, A., Aiba, M., Ando, M., Anten, N., Aspinwall, M. J., Baltzer, J. L., Baraloto, C., Battaglia, M., Battles, J. J., Bond-Lamberty, B., van Breugel, M., Camac, J., Claveau, Y., Coll, L., Dannoura, M., Delagrange, S., Domec, J.-C., Fatemi, F., Feng, W., Gargaglione, V., Goto, Y., Hagihara, A., Hall, J. S., Hamilton, S., Harja, D., Hiura, T., Holdaway, R., Hutley, L. S., Ichie, T., Jokela, E. J., Kantola, A., Kelly, J. W. G., Kenzo, T., King, D., Kloeppel, B. D., Kohyama, T., Komiyama, A., Laclau, J.-P., Lusk, C. H., Maguire, D. A., le Maire, G., Mäkelä, A., Markesteijn, L., Marshall, J., McCulloh, K., Miyata, I., Mokany, K., Mori, S., Myster, R. W., Nagano, M., Naidu, S. L., Nouvellon, Y., O'Grady, A. P., O'Hara, K. L., Ohtsuka, T., Osada, N., Osunkoya, O. O., Peri, P. L., Petritan, A. M., Poorter, L., Portsmuth, A., Potvin, C., Ransijn, J., Reid, D., Ribeiro, S. C., Roberts, S. D., Rodríguez, R., Saldaña-Acosta, A., Santa-Regina, I., Sasa, K., Selaya, N. G., Sillett, S. C., Sterck, F., Takagi, K., Tange, T., Tanouchi, H., Tissue, D., Umehara, T., Utsugi, H., Vadeboncoeur, M. A., Valladares, F., Vanninen, P., Wang, J. R., Wenk, E., Williams, R., de Aquino Ximenes, F., Yamaba, A., Yamada, T., Yamakura, T., Yanai, R. D., and York, R. A.: BAAD: a Biomass And Allometry Database for woody plants, Ecology, 96, 1445–1445, https://doi.org/10.1890/14-1889.1, 2015.

Forkel, M., Schmidt, L., Zotta, R.-M., Dorigo, W., and Yebra, M.: Estimating leaf moisture content at global scale from passive microwave satellite observations of vegetation optical depth, Hydrol. Earth Syst. Sci., 27, 39–68, https://doi.org/10.5194/hess-27-39-2023, 2023a.

Forkel, M., Andela, N., de Laat, J., Huijnen, V., Awotwi, A., Kinalczyk, D., Marrs, C., and Wessollek, C.: Sense4Fire ATBDv2.1. Sentinel-based fuel, fire and emissions products to constrain the changing role of vegetation fires in the global carbon cycle. Algorithm Theoretical Baseline Document Version 2.1, 2023b.

Forkel, M., Andela, N., de Laat, J., Huijnen, V., van Wees, D., Kinalczyk, D., Marrs, C., and Wessollek, C.: Sense4Fire PVRv3. Sentinel-based fuel, fire and emissions products to constrain the changing role of vegetation fires in the global carbon cycle. Product Validation Report Version 3, 2024.

Fuster, B., Sánchez-Zapero, J., Camacho, F., García-Santos, V., Verger, A., Lacaze, R., Weiss, M., Baret, F., and Smets, B.: Quality Assessment of PROBA-V LAI, fAPAR and fCOVER Collection 300 m Products of Copernicus Global Land Service, Remote Sens., 12, 1017, https://doi.org/10.3390/rs12061017, 2020.

Holland, E. A., Post, W. M., Matthews, E. G., Sulzman, J. M., Staufer, R., and Krankina, O. N.: A Global Database of Litterfall Mass and Litter Pool Carbon and Nutrients, , https://doi.org/10.3334/ORNLDAAC/1244, 2014.

de Laat, A., Huijnen, V., Andela, N., and Forkel, M.: Assessment of satellite observation-based wildfire emissions inventories using TROPOMI data and IFS-COMPO model simulations, EGUsphere, 1–81, https://doi.org/10.5194/egusphere-2024-732, 2024.

Lang, N., Jetz, W., Schindler, K., and Wegner, J. D.: A high-resolution canopy height model of the Earth, Nat. Ecol. Evol., 7, 1778–1789, https://doi.org/10.1038/s41559-023-02206-6, 2023.

Lizundia-Loiola, J., Otón, G., Ramo, R., and Chuvieco, E.: A spatio-temporal active-fire clustering approach for global burned area mapping at 250 m from MODIS data, Remote Sens. Environ., 236, 111493, https://doi.org/10.1016/j.rse.2019.111493, 2020.

Moesinger, L., Dorigo, W., Jeu, R. de, Schalie, R. van der, Scanlon, T., Teubner, I., and Forkel, M.: The global long-term microwave Vegetation Optical Depth Climate Archive (VODCA), Earth Syst. Sci. Data, 12, 177–196, https://doi.org/10.5194/essd-12-177-2020, 2020.

Rego, F. C., Morgan, P., Fernandes, P., and Hoffman, C.: Fire Science: From Chemistry to Landscape Management, Springer International Publishing, Cham, https://doi.org/10.1007/978-3-030-69815-7, 2021.

van der Schalie, R., de Jeu, R. A. M., Kerr, Y. H., Wigneron, J. P., Rodríguez-Fernández, N. J., Al-Yaari, A., Parinussa, R. M., Mecklenburg, S., and Drusch, M.: The merging of radiative transfer based surface soil moisture data from SMOS and AMSR-E, Remote Sens. Environ., 189, 180–193, https://doi.org/10.1016/j.rse.2016.11.026, 2017.

van Wees, D., van der Werf, G. R., Randerson, J. T., Rogers, B. M., Chen, Y., Veraverbeke, S., Giglio, L., and Morton, D. C.: Global biomass burning fuel consumption and emissions at 500 m spatial resolution based on the Global Fire Emissions Database (GFED), Geosci. Model Dev., 15, 8411–8437, https://doi.org/10.5194/gmd-15-8411-2022, 2022.

Yebra, M., Scortechini, G., Badi, A., Beget, M. E., Boer, M. M., Bradstock, R., Chuvieco, E., Danson, F. M., Dennison, P., Dios, V. R. de, Bella, C. M. D., Forsyth, G., Frost, P., Garcia, M., Hamdi, A., He, B., Jolly, M., Kraaij, T., Martín, M. P., Mouillot, F., Newnham, G., Nolan, R. H., Pellizzaro, G., Qi, Y., Quan, X., Riaño, D., Roberts, D., Sow, M., and Ustin, S.: Globe-LFMC, a global plant water status database for vegetation ecophysiology and wildfire applications, Sci. Data, 6, 1–8, https://doi.org/10.1038/s41597-019-0164-9, 2019.